

Evidence against manifest right-handed currents in neutron beta decay

A. García*

Departamento de Física, Centro de Investigación y de Estudios Avanzados del Instituto Politécnico Nacional, Apartado Postal 14-740, México, Distrito Federal, 07000, Mexico

G. Sánchez-Colón†

Departamento de Física Aplicada, Centro de Investigación y de Estudios Avanzados del Instituto Politécnico Nacional, Unidad Mérida, Apartado Postal 73, Cordemex, Mérida, Yucatán, 97310, Mexico

(Received 18 August 2009; revised manuscript received 8 January 2010; published 28 January 2010)

The bounds and presence of manifest right-handed currents in neutron beta decay are reviewed. Assuming the unitarity of the Cabibbo-Kobayashi-Maskawa matrix, the current experimental situation imposes very stringent limits on the mixing angle, $-0.00077 < \zeta < 0.00089$, and on the mass eigenstate, M_2 (GeV) \in (291.4, 439.9), in contradiction with the established lower bound on M_2 .

DOI: [10.1103/PhysRevD.81.014030](https://doi.org/10.1103/PhysRevD.81.014030)

PACS numbers: 13.30.Ce, 12.15.Ff, 12.60.-i, 23.40.Bw

I. INTRODUCTION

The standard model (SM) has its predictive power in neutron beta decay ($n\beta d$) afflicted by the fact that it has two free parameters, namely, V_{ud} and $\lambda = g_1/f_1$ (the ratio of the two leading form factors at zero momentum transfer). In order to make precise predictions, both parameters should be determined experimentally with great precision. The observables measured with the best precision in free $n\beta d$ are the transition rate R and the electron-neutron spin asymmetry α_e . In superallowed $n\beta d$ V_{ud} can be determined very precisely. At present, the problem is that measurements of α_e give two incompatible values. Despite this difficulty it is still possible to obtain precise predictions for the region of validity of the SM using the expressions of the SM for R and α_e (instead of their experimental values) and the unitarity of the Cabibbo-Kobayashi-Maskawa matrix along with the experimental values of V_{us} and V_{ud} . This analysis was carried out in Ref. [1], and the best prediction of the SM for free $n\beta d$ is given in Table II and depicted in Fig. 2(a) of this reference.

In this paper we want to extend this approach to study the bounds and the presence of right-handed currents [2] (RHCs) in $n\beta d$. Two new free parameters are introduced, the mixing angle ζ of W_L and W_R and the ratio of squares of the masses of the corresponding mass eigenstates $\delta = (M_1/M_2)^2$. In addition, we shall use the very precise current measurement of V_{ud} in nuclear physics, which as we shall see plays a very important role.

We have assumed that the Cabibbo-Kobayashi-Maskawa matrix is common to W_L and W_R . This is referred to as manifest RHCs [2].

II. EXPRESSIONS AND EXPERIMENTAL SITUATION

The SM predicts for the decay rate of $n\beta d$ the expression

$$R(10^{-3} \text{ s}^{-1}) = |V_{ud}|^2(0.1897)(1 + 3\lambda^2) \times (1 + 0.0739 \pm 0.0008) \quad (1)$$

at the level of a precision of 10^{-4} . The detailed derivation of Eq. (1) is found in Ref. [3]. The current experimental value of the neutron mean life [4] produces $R_{\text{exp}}(10^{-3} \text{ s}^{-1}) = 1.12905(132)$. The theoretical error in R of 0.0008 is included (recently this theoretical bias has been reduced [5,6]). In our analysis this theoretical error in R is folded into its experimental error bar; $\sigma_R = 0.00102$ becomes $\sigma'_R = 0.00132$ (in units of 10^{-3} s^{-1}). However, it must be stressed that our analysis is independent of R_{exp} and its error bar σ'_R and α_e . This is true even though the neutron mean life is not yet fully converged [7], and the reason for this is that the analysis of Sec. III to obtain the regions of validity of the SM and the SM with RHCs is based on the expressions of R and α_e instead of their experimental values.

The advantage of the integrated observables α_e , $\alpha_{e\nu}$, and α_ν is that their definitions entail only kinematics and do not assume any particular theoretical approach. The electron-neutrino angular correlation coefficient is defined as $\alpha_{e\nu} = 2[N(\theta_{e\nu} < \pi/2) - N(\theta_{e\nu} > \pi/2)]/[N(\theta_{e\nu} < \pi/2) + N(\theta_{e\nu} > \pi/2)]$, where $N(\theta_{e\nu} < \pi/2)$ [$N(\theta_{e\nu} > \pi/2)$] is the number of all events with electron-neutrino pairs emitted in directions that make an angle between them smaller (greater) than $\pi/2$. Similarly the electron-neutron spin asymmetry coefficient is defined as $\alpha_e = 2[N(\theta_e < \pi/2) - N(\theta_e > \pi/2)]/[N(\theta_e < \pi/2) + N(\theta_e > \pi/2)]$, where θ_e is the angle between the electron direction and the polarization direction of the neutron. An

*Deceased

†gsanchez@mda.cinvestav.mx

analogous definition is used for the neutrino-neutron spin asymmetry α_ν . Reference [8] provides the complete numerically integrated formulas for the decay rate and angular coefficients.

At the 10^{-4} level the SM predicts for the electron asymmetry the expression [9]

$$\alpha_e = \frac{-0.00021 + 0.2763\lambda - 0.2772\lambda^2}{0.1897 + 0.5692\lambda^2}. \quad (2)$$

We have chosen a negative sign for λ to conform with the convention of [4]. The important remark here is that there is no theoretical uncertainty in α_e at this level of precision. The reason for this is that the uncertainty introduced by the model dependence of the contributions of Z^0 to the radiative corrections is common to the numerator and denominator of α_e and cancels away at the 10^{-4} level.

The analysis that leads to Eq. (2) can be extended to the neutrino and electron-neutrino asymmetry coefficients,

$$\alpha_\nu = \frac{0.0003 - 0.3794\lambda - 0.2772\lambda^2}{0.1897 + 0.5692\lambda^2}, \quad (3)$$

$$\alpha_{e\nu} = \frac{0.1382 + 0.00054\lambda - 0.1393\lambda^2}{0.1897 + 0.5692\lambda^2}. \quad (4)$$

It must be stressed that the angular coefficients are free of a theoretical error at a level of precision of 10^{-4} . This accuracy is better than the current experimental precision that modern experiments allow. The effects of strong interactions, radiative corrections, and the recoil of the proton have been included [9].

It has remained customary to present experimental results for the old order zero angular coefficients after all the corrections contained in α_e , α_ν , and $\alpha_{e\nu}$, have been applied to the experimental analysis [4],

$$A_0 = -\frac{2\lambda(\lambda + 1)}{1 + 3\lambda^2}, \quad (5)$$

$$B_0 = \frac{2\lambda(\lambda - 1)}{1 + 3\lambda^2}, \quad (6)$$

$$a_0 = \frac{1 - \lambda^2}{1 + 3\lambda^2}. \quad (7)$$

Also, besides presenting results for A_0 it is customary to report directly the value for λ obtained from expression (5). Thus, the experimental value of λ is free of theoretical uncertainties at the 10^{-4} level. We use this value of λ in Eq. (2) to estimate the corresponding value of α_e and its error bar. By following a similar procedure with Eqs. (6), (3), (7), and (4), we obtain the numerical values of α_ν and $\alpha_{e\nu}$.

From present experimental results [4] for the $n\beta d$ order zero angular coefficients, B_0 , a_0 , and A_0 , the corresponding experimental values of the integrated angular coefficients are $\alpha_\nu^{\text{exp}} = 0.9810(30)$, $\alpha_{e\nu}^{\text{exp}} = -0.0772(29)$, and the

two conflicting values for α_e , $\alpha_e^{\text{exp}}(\text{A}) = -0.08809(52)$ [10,11] and $\alpha_e^{\text{exp}}(\text{LYB}) = -0.08489(65)$ [12–14].

The expressions of the observables in free $n\beta d$ of the SM including the contributions of RHCs with a precision of 10^{-4} can be expressed as

$$R = (1.0739)A_\alpha V_{\text{ud}}^2(0.1897 + (0.5692)B_\alpha\lambda^2), \quad (8)$$

$$\alpha_e = \frac{D_\alpha(-0.00021 - (0.2763)F_\alpha\lambda - (0.2772)E_\alpha\lambda^2)}{A_\alpha(0.1897 + (0.5692)B_\alpha\lambda^2)}, \quad (9)$$

$$\alpha_\nu = \frac{D_\alpha(0.0003 - (0.3794)F_\alpha\lambda + (0.3795)E_\alpha\lambda^2)}{A_\alpha(0.1897 + (0.5692)B_\alpha\lambda^2)}, \quad (10)$$

$$\alpha_{e\nu} = \frac{0.1382 + (0.00054)C_\alpha\lambda - (0.1393)B_\alpha\lambda^2}{0.1897 + (0.5692)B_\alpha\lambda^2}. \quad (11)$$

Here [2], $A_\alpha \dots F_\alpha$ contain the corrections due to RHCs. $A_\alpha = 2(\eta_{\text{AV}}^2 + 1)/(\eta_{\text{AA}}^2 + 2\eta_{\text{AV}}^2 + 1)$, $B_\alpha = (\eta_{\text{AA}}^2 + \eta_{\text{AV}}^2)/(\eta_{\text{AV}}^2 + 1)$, $C_\alpha = (\eta_{\text{AA}} + \eta_{\text{AV}}^2)/(\eta_{\text{AV}}^2 + 1)$, $D_\alpha = -4\eta_{\text{AV}}/(\eta_{\text{AA}}^2 + 2\eta_{\text{AV}}^2 + 1)$, $E_\alpha = \eta_{\text{AA}}$, $F_\alpha = (\eta_{\text{AA}} + 1)/2$, where $\eta_{\text{AA}} = (\delta + \epsilon^2)/(\delta\epsilon^2 + 1)$, $\eta_{\text{AV}} = -(1 - \delta)\epsilon/(\delta\epsilon^2 + 1)$, with $\epsilon = (1 + \tan\zeta)/(1 - \tan\zeta)$. The numerical coefficients remain the same as in Eqs. (1)–(4).

III. DETERMINATION OF THE REGIONS OF VALIDITY

The region where the SM and the SM with RHCs (SMR and RHCR, respectively) remain valid at a 90% CL are determined by forming a χ^2 function with the sum of six terms, $((R_{\text{exp}} - R)/\sigma'_R)^2$, $((\alpha_e^{\text{exp}} - \alpha_e)/\sigma_{\alpha_e(\text{LYB})})^2$, $((\alpha_\nu^{\text{exp}} - \alpha_\nu)/\sigma_{\alpha_\nu})^2$, $((\alpha_{e\nu}^{\text{exp}} - \alpha_{e\nu})/\sigma_{\alpha_{e\nu}})^2$, $((V_{\text{us}}^{\text{exp}} - V_{\text{us}}A_\alpha^{1/2})/\sigma_{V_{\text{us}}})^2$, and $((V_{\text{ub}}^{\text{exp}} - V_{\text{ub}}A_\alpha^{1/2})/\sigma_{V_{\text{ub}}})^2$, where $V_{\text{ub}} = \sqrt{1 - V_{\text{ud}}^2 - V_{\text{us}}^2}$, and then minimizing the χ^2 at a lattice of points $(\alpha_e^{\text{exp}}, R_{\text{exp}})$ within a rectangle that covers $\pm 3\sigma'_R$ around R_{exp} and a range for α_e^{exp} covering $\alpha_e^{\text{exp}}(\text{A})$ and $\alpha_e^{\text{exp}}(\text{LYB})$. The values of σ'_R and $\sigma_{\alpha_e(\text{LYB})}$ can also be reduced from their current values of $0.00132 \times 10^{-3} \text{ s}^{-1}$ and 0.00065 to one-tenth of these values which run into the theoretical error bars of 10^{-4} . The free parameters varied at each $(\alpha_e^{\text{exp}}, R_{\text{exp}})$ point are λ , V_{ud} , and V_{us} for the SMR and λ , V_{ud} , V_{us} , ζ , and δ for the RHCR. In addition, we shall add a seventh constraint $((V_{\text{ud}}^{\text{exp}}(\text{NP}) - V_{\text{ud}}A_\alpha^{1/2})/\sigma_{V_{\text{ud}}})^2$ to χ^2 which incorporates the experimental nuclear physics (NP) value of $V_{\text{ud}}^{\text{exp}}(\text{NP}) = 0.97418(27)$.

The numerical results are displayed in Table I without the $V_{\text{ud}}^{\text{NP}}$ constraint and in Table II with the $V_{\text{ud}}^{\text{NP}}$ constraint included. The corresponding 90% CL SMR and RHCR are depicted in Figs. 1 and 2.

TABLE I. The minimum of χ^2 , its corresponding value of α_e , the prediction for α_ν , and the partial contribution from α_ν to χ^2 for seven values of R_{exp} (in units of 10^{-3} sec^{-1}) without the $V_{\text{ud}}^{\text{NP}}$ constraint. The upper numbers obey the constraint of α_ν^{exp} and the lower ones do not obey it. The last two columns give the 90% CL bounds on the two free parameters of manifest RHCs, ζ and δ , respectively.

R	SM				RHCs					
	Value α_e	χ^2	Prediction α_ν	$\chi^2(\alpha_\nu)$	Value α_e	χ^2	Prediction α_ν	$\chi^2(\alpha_\nu)$	ζ	Parameters $\delta = (M_1/M_2)^2$
1.133 01	-0.087 72	5.32	0.987 59	4.82	-0.084 97	10^{-5}	0.981 00	10^{-7}	(-0.009 24, -0.002 63)	(0.0384, 0.0812)
	-0.087 72	0.50			-0.084 97	10^{-6}			(-0.009 53, 0.008 84)	(-0.2560, 0.1662)
1.131 69	-0.087 52	5.33	0.987 65	4.92	-0.084 97	10^{-4}	0.981 00	10^{-7}	(-0.008 56, -0.001 95)	(0.0380, 0.0808)
	-0.087 49	0.41			-0.084 97	10^{-5}			(-0.008 90, 0.009 53)	(-0.2624, 0.1645)
1.130 37	-0.087 26	5.35	0.987 72	5.02	-0.084 92	10^{-5}	0.981 00	10^{-7}	(-0.008 01, -0.001 40)	(0.0378, 0.0804)
	-0.087 23	0.33			-0.084 92	10^{-7}			(-0.008 39, 0.010 22)	(-0.2701, 0.1636)
1.129 05	-0.087 00	5.38	0.987 79	5.12	-0.084 87	10^{-5}	0.981 00	10^{-7}	(-0.007 46, -0.000 84)	(0.0377, 0.0802)
	-0.087 00	0.25			-0.084 87	10^{-6}			(-0.007 88, 0.010 95)	(-0.2782, 0.1626)
1.127 73	-0.086 79	5.42	0.987 86	5.23	-0.084 83	10^{-5}	0.981 00	10^{-8}	(-0.006 91, -0.000 29)	(0.0375, 0.0799)
	-0.086 76	0.19			-0.084 83	10^{-6}			(-0.007 38, 0.011 68)	(-0.2867, 0.1617)
1.126 41	-0.086 53	5.47	0.987 93	5.33	-0.084 79	10^{-5}	0.981 00	10^{-7}	(-0.006 33, 0.000 29)	(0.0372, 0.0796)
	-0.086 50	0.14			-0.084 79	10^{-5}			(-0.006 86, 0.012 51)	(-0.2956, 0.1607)
1.125 09	-0.086 27	5.53	0.987 99	5.44	-0.084 73	10^{-6}	0.981 00	10^{-9}	(-0.005 81, 0.000 82)	(0.0371, 0.0794)
	-0.086 27	0.09			-0.084 73	10^{-6}			(-0.006 38, 0.013 29)	(-0.3055, 0.1599)

IV. DISCUSSION

In Table I the constraint of $V_{\text{ud}}^{\text{NP}}$ is not enforced, while in Table II this constraint is operative. In both tables in each entry the upper numbers obey the constraint of α_ν^{exp} and the lower ones do not obey it. The last two columns give the 90% CL bounds on the two free parameters of manifest RHCs.

The χ^2 of the SM predictions in both tables show a discrepancy of 2.2 standard deviation. One can see that such a discrepancy is saturated by $\chi^2(\alpha_\nu)$. The presence or

absence of the $V_{\text{ud}}^{\text{NP}}$ constraint plays no role in this discrepancy. When RHCs are allowed in, one can appreciate the relevance of $V_{\text{ud}}^{\text{NP}}$. The bounds on ζ are reduced and made very uniform when $V_{\text{ud}}^{\text{NP}}$ constrains χ^2 . The ranges for ζ in Table I are negative at the top five entries and only in the last two at the bottom $\zeta = 0$ is allowed. The length $\Delta\zeta$ of these ranges is around 0.006 60. In contrast, in Table II the ranges for ζ are quite symmetric around $\zeta = 0$ and have $\Delta\zeta$ of 0.001 66, approximately one-fourth of the length when $V_{\text{ud}}^{\text{NP}}$ is not operative. One can also see in the lower numbers that whether α_ν^{exp} is enforced or not makes no

TABLE II. The minimum of χ^2 , its corresponding value of α_e , the prediction for α_ν , and the partial contribution from α_ν to χ^2 for seven values of R_{exp} (in units of 10^{-3} sec^{-1}) with the $V_{\text{ud}}^{\text{NP}}$ constraint. The upper numbers obey the constraint of α_ν^{exp} and the lower ones do not obey it. The last two columns give the 90% CL bounds on the two free parameters of manifest RHCs, ζ and δ , respectively.

R	SM				RHCs					
	Value α_e	χ^2	Prediction α_ν	$\chi^2(\alpha_\nu)$	Value α_e	χ^2	Prediction α_ν	$\chi^2(\alpha_\nu)$	ζ	Parameters $\delta = (M_1/M_2)^2$
1.133 01	-0.087 78	5.34	0.987 58	4.81	-0.087 17	0.51	0.981 00	10^{-8}	(-0.000 785, 0.000 890)	(0.0318, 0.0754)
	-0.087 75	0.52			-0.087 17	0.51			(-0.000 769, 0.000 892)	(-0.1011, 0.0997)
1.131 69	-0.087 52	5.35	0.987 65	4.91	-0.086 94	0.42	0.981 04	10^{-4}	(-0.000 784, 0.000 891)	(0.0320, 0.0755)
	-0.087 52	0.43			-0.086 94	0.42			(-0.000 768, 0.000 892)	(-0.1007, 0.0992)
1.130 37	-0.087 26	5.36	0.987 72	5.01	-0.086 68	0.34	0.981 02	10^{-5}	(-0.000 784, 0.000 891)	(0.0327, 0.0758)
	-0.087 26	0.35			-0.086 68	0.34			(-0.000 784, 0.000 893)	(-0.1014, 0.1000)
1.129 05	-0.087 05	5.40	0.987 78	5.11	-0.086 42	0.26	0.981 00	10^{-7}	(-0.000 768, 0.000 891)	(0.0334, 0.0761)
	-0.087 02	0.27			-0.086 42	0.26			(-0.000 768, 0.000 894)	(-0.1020, 0.1005)
1.127 73	-0.086 79	5.44	0.987 85	5.22	-0.086 19	0.20	0.981 02	10^{-5}	(-0.000 767, 0.000 892)	(0.0337, 0.0762)
	-0.086 79	0.21			-0.086 19	0.20			(-0.000 767, 0.000 894)	(-0.1019, 0.1004)
1.126 41	-0.086 53	5.49	0.987 92	5.32	-0.085 96	0.15	0.981 04	10^{-4}	(-0.000 766, 0.000 893)	(0.0341, 0.0764)
	-0.086 53	0.15			-0.085 96	0.14			(-0.000 766, 0.000 895)	(-0.1018, 0.1003)
1.125 09	-0.086 32	5.55	0.987 99	5.43	-0.085 70	0.10	0.981 02	10^{-5}	(-0.000 766, 0.000 894)	(0.0347, 0.0767)
	-0.086 29	0.11			-0.085 70	0.10			(-0.000 766, 0.000 895)	(-0.1024, 0.1009)

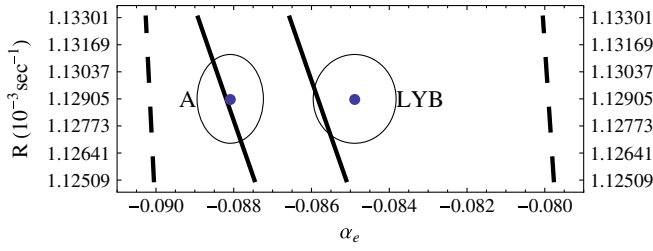


FIG. 1 (color online). The 90% CL SMR (solid lines) and RHCR (dashed lines) without the V_{ud}^{NP} constraint included. The 90% CL region around the current central values of α_e^{exp} and R_{exp} are also displayed.

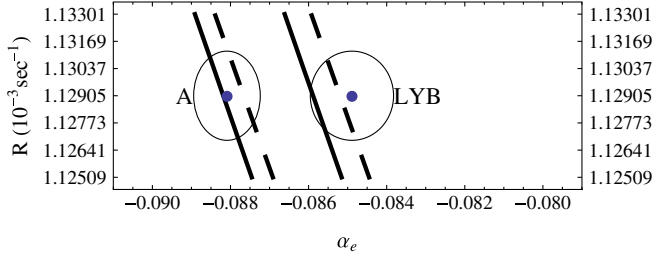


FIG. 2 (color online). The 90% CL SMR (solid lines) and RHCR (dashed lines) with the V_{ud}^{NP} constraint included. The 90% CL region around the current central values of α_e^{exp} and R_{exp} are also displayed.

difference. One can, then, conclude that the bounds of ζ , typically of

$$\zeta \in (-0.00077, 0.00089) \quad (12)$$

are imposed solely by V_{ud}^{NP} , V_{us} , and the unitarity of the Cabibbo-Kobayashi-Maskawa matrix. These bounds may be compared with previous ones. In Ref. [15] one had $\zeta \in$

$(-0.00060, 0.00280)$ with a $\Delta\zeta = 0.0340$. The range (12) is more symmetric and has half the length.

The bounds on δ are practically independent of V_{ud}^{NP} , but they are very dependent on α_ν^{exp} as can be seen by comparing the upper and the lower numbers. Actually, the upper bound on δ , at around 0.076, is also almost independent of α_ν^{exp} . It is the lower bound on δ that is very sensitive on α_ν^{exp} . In Table II it varies from about $\delta \approx 0.033 > 0$ to about $\delta \approx -0.1020 < 0$, according to whether α_ν^{exp} is operative or not. Of course, a negative δ is meaningless and the actual lower bound should be $\delta = 0$, which makes the range for δ an upper bound only. One can conclude that α_ν^{exp} imposes the 90% CL range of

$$\delta \in (0.0334, 0.0761) \quad (13)$$

upon δ .

At this point one should translate (13) into a range for M_2 . One has

$$M_2 \text{ (GeV)} \in (291.4, 439.9). \quad (14)$$

Range (14) shows vividly how effective α_ν is for setting an upper bound on M_2 . It also means that manifest RHCs are detected in $n\beta d$. However, one already knows that lower bounds on M_2 have been established. At present one may accept as a conservative lower bound $M_2 > 715$ GeV [4]. This is in clear contradiction with range (14).

In order to better understand this situation we have prepared another table, Table III. We are interested in appreciating what refined measurements of α_ν^{exp} may produce in, hopefully, the near future. We assume that the error bar σ_{α_ν} is reduced to one-tenth of its current value. That is, we assume $\sigma_{\alpha_\nu} = 0.00030$ and we vary the central value α_ν^{exp} from 0.98100 to 0.98760. We keep R_{exp} , V_{ud}^{exp} (NP), and V_{us}^{exp} at their current central values and error

TABLE III. The minimum of χ^2 , its corresponding value of α_e , the prediction for α_ν , and the partial contribution from α_ν to χ^2 for several values of α_ν^{exp} with the error bar σ_{α_ν} reduced to one-tenth of its current value. R_{exp} , V_{ud}^{exp} (NP), and V_{us}^{exp} are kept at their current central values and error bars. The last three columns give the 90% CL bounds on the two free parameters of manifest RHCs, ζ and δ , and the corresponding bounds on M_2 , respectively.

α_ν	SM				RHCs							
	Value α_e	Value χ^2	Prediction α_ν	Prediction $\chi^2(\alpha_\nu)$	Value α_e	Value χ^2	Prediction α_ν	Prediction $\chi^2(\alpha_\nu)$	Parameters		Bounds	
									ζ	$\delta = (M_1/M_2)^2$	M_2 (GeV)	
0.9810	-0.08840	482.99	0.98740	454.85	-0.08642	0.26	0.9810	10^{-9}	(-0.000768, 0.000891)	(0.0564, 0.0609)	(325.8, 338.5)	
0.9816	-0.08827	401.45	0.98743	378.08	-0.08648	0.26	0.9816	10^{-8}	(-0.000767, 0.000891)	(0.0536, 0.0583)	(332.9, 347.2)	
0.9822	-0.08817	327.38	0.98747	308.23	-0.08653	0.26	0.9822	10^{-8}	(-0.000767, 0.000890)	(0.0507, 0.0556)	(340.9, 357.0)	
0.9828	-0.08804	260.98	0.98750	245.69	-0.08658	0.26	0.9828	10^{-7}	(-0.000766, 0.000889)	(0.0476, 0.0528)	(349.8, 368.5)	
0.9834	-0.08791	202.05	0.98754	190.19	-0.08663	0.26	0.9834	10^{-7}	(-0.000766, 0.000889)	(0.0443, 0.0498)	(360.2, 381.9)	
0.9840	-0.08780	150.65	0.98757	141.71	-0.08668	0.26	0.9840	10^{-7}	(-0.000765, 0.000888)	(0.0407, 0.0467)	(372.0, 398.5)	
0.9846	-0.08767	106.80	0.98761	100.40	-0.08674	0.26	0.9846	10^{-7}	(-0.000765, 0.000887)	(0.0368, 0.0433)	(386.3, 419.1)	
0.9852	-0.08754	70.49	0.98764	66.20	-0.08679	0.26	0.9852	10^{-7}	(-0.000764, 0.000887)	(0.0324, 0.0396)	(404.0, 446.6)	
0.9858	-0.08741	41.72	0.98768	39.09	-0.08684	0.26	0.9858	10^{-7}	(-0.000764, 0.000886)	(0.0273, 0.0355)	(426.7, 486.5)	
0.9864	-0.08731	20.49	0.98771	19.05	-0.08689	0.26	0.9864	10^{-7}	(-0.000763, 0.000885)	(0.0211, 0.0310)	(456.6, 553.4)	
0.9870	-0.08718	6.80	0.98774	6.15	-0.08694	0.26	0.9870	10^{-7}	(-0.000762, 0.000886)	(0.0119, 0.0256)	(502.4, 736.9)	
0.9876	-0.08705	0.65	0.98778	0.35	-0.08702	0.26	0.9876	10^{-7}	(-0.000758, 0.000884)	(-0.0187, 0.0187)	>587.9	

bars. The results are displayed in Table III, in steps of 0.000 60.

As can be seen in the last column of Table III, at the 90% CL only when the experimental value of α_ν is greater than 0.9870 the upper bound obtained for M_2 is not ruled out by its present established lower bound. For $\alpha_\nu^{\text{exp}} \geq 0.9876$ the central value for δ is compatible with zero. One can conclude that a clean signal of manifest RHCs can be obtained only if future measurements of α_ν^{exp} find it in the range

$$\alpha_\nu^{\text{exp}} \in (0.9870, 0.9876). \quad (15)$$

V. CONCLUSIONS

The current experimental situation in $n\beta d$ and in the lower bounds on M_2 leads one to conclude that manifest RHCs run into a contradiction, which leads one to conclude that manifest RHCs are strongly eliminated as a

possibility of physics beyond the SM. The experimental quantity which leads to this conclusion is the current value of α_ν .

However, future refined experiments may correct the current situation provided two conditions are met: (1) α_ν is found within range (15) and (2) α_e is found in the future in the range $\alpha_e^{\text{exp}} \in (-0.085\,70, -0.087\,17)$ of Table II. If either of these conditions fail, then manifest RHCs will be strongly eliminated. Of course, other forms of new physics could be detected by α_ν , as can be appreciated by the values of χ^2 in the SM case in Table III.

As a final remark, it is not idle to emphasize the importance of refined very precise measurements of the observables in $n\beta d$.

ACKNOWLEDGMENTS

The authors would like to thank CONACyT (México) for partial support.

-
- [1] A. García and G. Sánchez-Colón, *Phys. Rev. D* **77**, 073005 (2008).
 - [2] M. A. B. Bég *et al.*, *Phys. Rev. Lett.* **38**, 1252 (1977).
 - [3] A. García, J. L. García-Luna, and G. López Castro, *Phys. Lett. B* **500**, 66 (2001).
 - [4] C. Amsler *et al.* (Particle Data Group), *Phys. Lett. B* **667**, 1 (2008).
 - [5] A. Czarnecki, W. J. Marciano, and A. Sirlin, *Phys. Rev. D* **70**, 093006 (2004).
 - [6] W. J. Marciano and A. Sirlin, *Phys. Rev. Lett.* **96**, 032002 (2006).
 - [7] A. Serebrov *et al.*, *Phys. Lett. B* **605**, 72 (2005).
 - [8] A. García and P. Kielanowski, *The Beta Decay of Hyperons*, Lecture Notes in Physics Vol. 222 (Springer-Verlag, Berlin, 1985).
 - [9] J. L. García-Luna and A. García, *J. Phys. G* **32**, 333 (2006).
 - [10] H. Abele *et al.*, *Phys. Rev. Lett.* **88**, 211801 (2002).
 - [11] H. Abele, *Prog. Part. Nucl. Phys.* **60**, 1 (2008).
 - [12] P. Liaud, *Nucl. Phys.* **A612**, 53 (1997).
 - [13] B. Yerozolimsky *et al.*, *Phys. Lett. B* **412**, 240 (1997).
 - [14] P. Bopp *et al.*, *Phys. Rev. Lett.* **56**, 919 (1986).
 - [15] M. Aquino, A. Fernandez, and A. García, *Phys. Lett. B* **261**, 280 (1991).